International Journal of Research
Available at https://edupediapublications.org/journals
e-ISSN: 2348-6848
p-ISSN: 2348-795X
Volume 05 Issue 12
April 2018

A High Gain DC-DC Converter with Soft Switching For Inverter with Grid Connected Unit

Shabana Begum , Dr. .P.Mallikarjun Sharma , Dr.P.Sridhar

M-tech Student Scholar Department of Power Electronics and Electrical Drives, Institute of Aeronautical Engineering, Dundigal, Hyderabad, Telangana, India.
Email: shabana22614@gmail.com

Professor Department of Power Electronics and Electrical Drives, Institute of Aeronautical Engineering, Dundigal, Hyderabad, Telangana, India.
Email: p.mallikarjunsharma@iare.ac.in

Department of Power Electronics & Electrical Drives, (H.O.D) Institute of Aeronautical Engineering (IARE) , Dundigal, Hyderabad; Telangana, India
Email:Sridhar@iare.ac.in

Abstract- *A soft-switching dc/dc converter with high voltage gain is proposed in this paper. It provides a continuous input current and high voltage gain. Moreover, soft-switching characteristic of the proposed converter reduces switching loss of active power switches and raises the conversion efficiency. The reverse-recovery problem of output rectifiers is also alleviated by controlling the current changing rates of diodes with the use of the leakage inductance of a coupled inductor. Hybrid power system consists of a combination of renewable energy sources such as: photovoltaic (PV), wind generators, hydro, etc., to charge batteries and provide power to meet the energy demand. Finally, a simplified design procedure is proposed in hybrid system by using inverter with grid connected unit.*

Index Terms— Soft Switching, Boost converter, High voltage gain, Hybrid power system (photo voltaic, wind generators, hydroelectric systems), stand-alone system.

1. INRODUCTION

Recently, the demand for dc/dc converters with high voltage gain has increased. The energy shortage and the atmosphere pollution have led to more researches on the renewable and green energy sources such as the solar arrays and the fuel cells. Moreover, the power systems based on battery sources and super capacitors have been increased. Unfortunately, the output voltages of these sources are relatively low. Therefore, the step-up power conversion is required in these systems. Besides the step-up function, the demands such as low current ripple, high efficiency, fast dynamics, light weight, and high power density have also increased for various applications. Input current ripple is an important factor in a high step-up dc/dc converter [5]. Especially in the fuel cell systems, reducing the input current ripple is very important because the large current ripple shortens fuel cell's lifetime as well as decreases performances. Therefore, current fed converters are commonly used due to their ability to reduce the current ripple. In applications that require a voltage step-up function and a continuous input current, a continuous conduction-mode (CCM) boost converter [3][4] is often used due to its advantages such as continuous input current and simple structure. However, it has a limited voltage gain due to its parasitic components.

The reverse-recovery problem of the output diodes is another important factor in dc/dc converters with high voltage gain. In order to overcome these problems, various topologies have been introduced. In order to extend the voltage gain, the boost converters with coupled inductors are proposed[2]. Their voltage gains are extended, but they lose a continuous input current characteristic and the efficiency is degraded due to hard switching's of power switches. For a continuous input current, current-fed step-up converters are proposed.

They provide high voltage gain[1] and galvanic isolation. However, the additional snubbers are required to reduce the voltage stresses of switches. In order to increase the efficiency[6][7] and power conversion density, a soft-switching technique is required in dc/dc converters.

Increasing population growth and economic development are accelerating the rate at which energy and in particular electrical energy is being demanded. All methods of electricity generation have consequences for the environment, so meeting this growth in demand, while safe- guarding the environment poses a growing challenge. Renewable energy technology offers the promise of clean, abundant energy gathered from self-renewing resources such as sun, wind, water, earth and plants. Virtually all regions of the world have renewable resources of one type or another. Renewable energy

technology offer important benefits compared to those of conventional energy sources.

Hybrid power systems consists of a combination of renewable energy sources such as: photovoltaic (PV), wind generators, hydro, etc., to charge batteries and provide power to meet the energy demand, considering the local geography and other details of the place of installation. These types of systems, which are not connected to the main utility grid, are also used in stand-alone applications and operate independently and reliably. The best applications for these systems are in remote places, such as rural villages, in telecommunications, etc.

2 Overview of High Voltage Gain Dc–Dc Converter Topologies

The converters shown in Fig.1 depict some of the high voltage gain topologies that are representative of the existing configurations. Direct voltage step up using high frequency transformer renders a simple and easily controllable converter providing high gain. Isolated current-fed dc–dc converters [Fig 1(a)] [7]–[9] are example of this category. However, these topologies result in high voltage spikes across the switch (due to leakage inductance) and large ripple in primary side transformer current as the turns ratio in the high frequency transformer increases. The isolated systems are relatively costly, bulky, and generally less efficient [10] even though they offer more safety, eliminate issues such as ground leakage current and can provide multiple outputs among other advantages.

Most of the nonisolated high voltage gain dc–dc power converters employ coupled inductor (to achieve higher voltage gain) [Fig. 1(b)] [11] in contrast to a high frequency transformer used by the isolated versions [Fig. 1(a)]. The coupled inductor-based dc–dc converter has advantages over isolated transformer-based dc–dc converter in minimizing current stress, using lower rating components and simple winding structure. Modeling procedure of the coupled inductor is described in [12]. For high power converter applications, interleaved coupled inductor-based boost converters [13]–[15] have also been proposed [Fig.1(c)].

A demerit of coupled inductor-based systems is that they have to deal with higher leakage inductance, which causes voltage spikes across the main switch during turn-OFF time and current spike during turn-ON time, resulting in a reduction of the overall circuit efficiency. The effects of leakage inductance can be eliminated by using an active clamp network shown in Fig. 1(d) [9], [15], which provides an alternate path to recover leakage energy. But active clamp network is not as efficient as a passive clamp because of conduction losses across the power switch of the active clamp [16] network. Active clamp network consists of a switch with passive components while passive clamp network [Fig. 1(e)] [4] consists of passive components such as diode, capacitor, and resistor. The passive clamp circuit is more popular to reduce voltage stress across the converter switch by recycling leakage energy [17].

The energy recovered from the leakage inductance can be calculated from the following equation:

$$\frac{1}{2}L_{lk}I_L^2 \tag{1}$$

where Llk is the leakage inductance, IL is the inductor current, and Lm is the magnetizing inductance given by

$$L_{lk} = (1-k)\,L; L_m = kL \tag{2}$$

where k is the coupling coefficient and L is the inductance. Voltage across clamp capacitor C can be calculated from (1)

$$\frac{1}{2}L_{lk}I_L^2 = \frac{1}{2}CV_C^2 \tag{3}$$

where C and VC are the clamping capacitance and clamp voltage, respectively.

Voltage gain of the converter can be increased without increasing the duty cycle of the switch by connecting an intermediate capacitor in series with the inductor [Fig. 2(f)] [6], [18], [19]. The intermediate energy storage capacitor with coupled inductor charges in parallel and discharges in series with the coupled inductor secondary.

Various principles discussed in preceding paragraphs have also been used in combinations to achieve high voltage gain and enhanced features [20]. A coupled inductor type boost converter has been used in association with a passive clamp circuit to achieve high gain and increased efficiency [4]. Converter configurations with coupled inductor in association with a voltage multiplier circuit [21] and/or intermediate capacitor [22], [23] have also been reported to achieve high voltage gain. In recent times, use of coupled inductors along with intermediate capacitors has also become popular [19].

International Journal of Research
Available at https://edupediapublications.org/journals
e-ISSN: 2348-6848
p-ISSN: 2348-795X
Volume 05 Issue 12
April 2018

Keeping in mind the merits and demerits of the various schemes described in preceding paragraphs, a novel topology has been proposed in this paper that achieves high voltage through a coupled inductor connected in interleaved manner that charges an intermediate buffer capacitor and a passive clamp network to recover the leakage energy. Coupled inductor leads to the incorporation of "turns ratio" into the gain expression that leads to high efficiency without increasing the duty ratio. As compared to existing high-gain dc–dc converters, the number of passive components used in the proposed converter is less, which reduces the cost and improves the efficiency. Though the proposed converter is applicable to any low voltage source application (e.g., solar PV, fuel cell stack, battery, etc.), this project focuses only on the solar PV source.

3 DESCRIPTION OF THE PROPOSED CONVERTER

Energy conversion efficiency of solar PV is quite low (about 12%–25%) [24]. Therefore, it is essential to use a highly efficient power conversion system to utilize the PV generated power to the maximum.

The proposed high-gain dc–dc converter configuration is shown in Fig. It consists of one passive clamp network, a coupled inductor (L_1, L_2), and an intermediate capacitor apart from other components. The symbol VPV represents the PV voltage applied to the circuit. S is the main switch of the proposed converter. The coupled inductor's primary and secondary inductors are denoted by L_1 and L_2. C_1 and D_1 represent the passive clamp network across L_1.

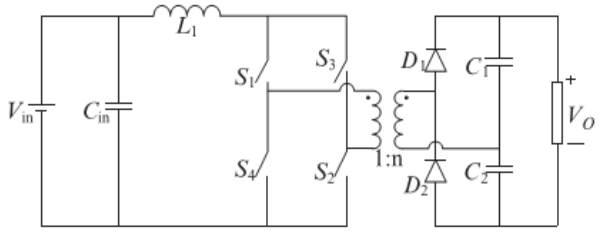

(a)

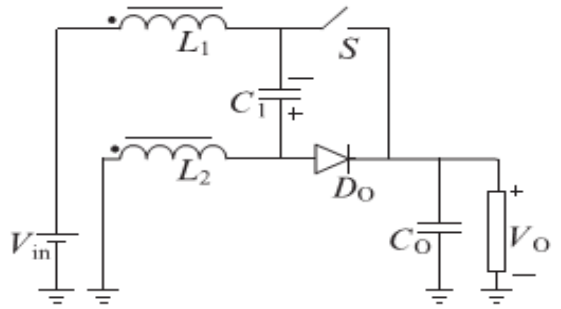

(b)

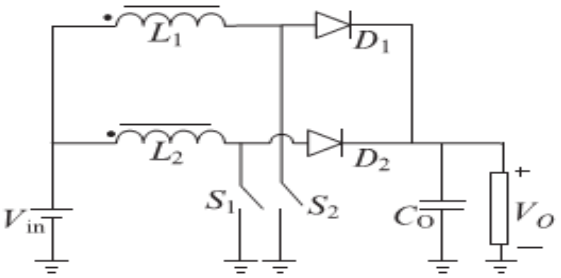

(c)

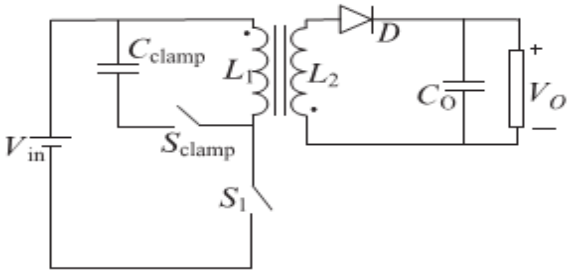

(d)

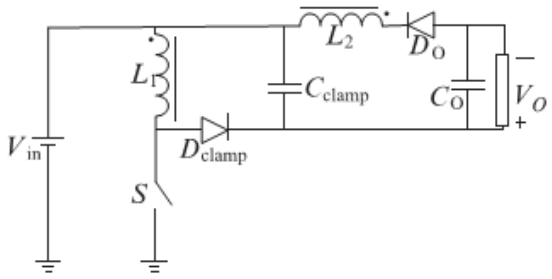

(e)

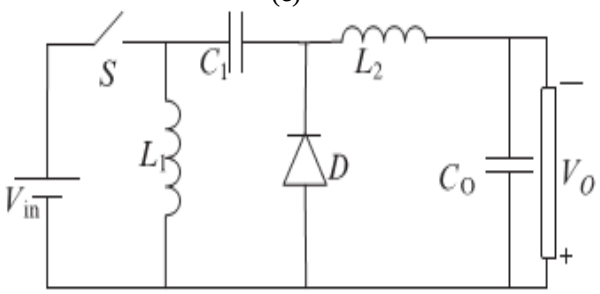

(f)

International Journal of Research
Available at https://edupediapublications.org/journals
e-ISSN: 2348-6848
p-ISSN: 2348-795X
Volume 05 Issue 12
April 2018

Fig.1. Circuit diagrams of the high voltage gain dc–dc converters: (a) isolated current-fed boost converter [8]; (b) coupled inductor boost converter [11]; (c) interleaved coupled inductor boost converter [14]; (d) active clamp converter [9]; (e) passive clamp converter [4]; and (f) intermediate energy storage capacitor-based converter [18].

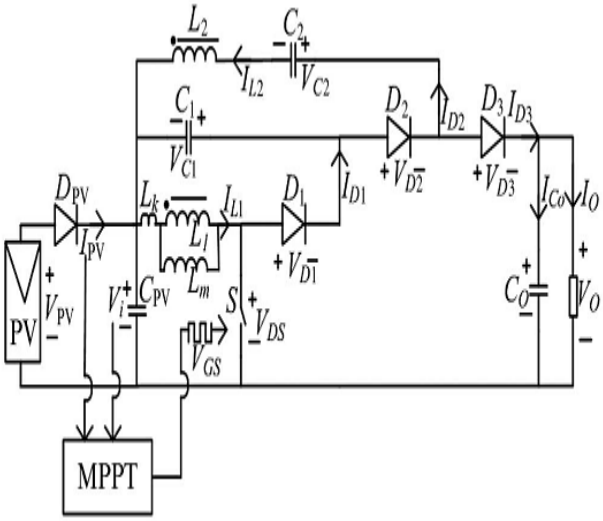

Fig.2. Circuit diagram of proposed dc–dc converter

The capacitor CO is the output capacitor while D3 is the output diode. The voltage VO is the average (dc) output across the load. The intermediate energy storage capacitor C2 and the feedback diode D2 are connected on the secondary side. The gain ratio n is given by

$$n = \frac{V_{L2}}{V_{L1}} \tag{4}$$

where VL1 and VL2 represent the voltages across inductors L1 and L2.

The operating modes for continuous conduction mode (CCM) are shown in Fig. Various operating modes are described below.

Mode 1 [$t_0 - t_1$]: The switch (S) is turned ON at the start of the converter operation. The current flows through the switch and the primary side of the coupled inductor (L_1), energizing the magnetizing inductance (Lm) of the coupled inductor. The current path is as shown in Fig. 3(a). The two diodes D_1 and D_3 are reverse biased, while D2 is forward biased during this mode. The intermediate capacitor C_2 is charged through D_2 by L_2 and capacitor C_1. If voltage across intermediate capacitor (C_2) becomes equal to the summation of voltages across L_2 and C_1, diode D_2 turns OFF. The current flowing through Lm(iLm) in this mode may be obtained by using the following relation:

$$i_{Lm}(t) = \frac{V_i}{L_m + L_k}(t - t_0) + i_{Lm}(t_0) \tag{5}$$

Mode 2 [$t_1 - t_2$]: This mode begins by turning OFF the main switch S. The parasitic capacitance of the switch S is charged by the magnetizing current flowing through the inductor L_1. The diode D_2 remains forward biased and current continues to flow through this. Current path in this mode is shown in Fig.4(b). The magnetizing inductance current for this mode is given by the following equation:

$$i_{Lm}(t) = \frac{V_i}{L_m + L_k}(t - t_1) + i_{Lm}(t_1) \tag{6}$$

Mode 3 [$t_2 - t_3$]: In this mode, diodes D_1 and D_3 become forward biased. D_2 is reverse biased and its current becomes zero in this mode. The leakage energy stored in the primary side of the coupled inductor (L_1) is recovered and stored in the clamp capacitor (C_1) through D_1. Also, the energy is transferred from the input side to the output side through diode D3 as shown in Fig. 4(c). The recovered leakage inductance current (iLk) is given by

$$i_{Lk}(t) = \frac{V_{C1}}{L_m + L_k}(t - t_2) + i_{Lm}(t_2) \tag{7}$$

Mode 4 [$t_3 - t_4$]: This mode begins after the completion of recovery of the leakage energy from inductor L_1. The diode D_1 now becomes reverse biased while diode D_3 remains forward biased in this mode. The current flows from the input side to the output side to supply the load as shown in Fig.4(d). The current iLm flowing through secondary inductor (L_2) is given by the following equation:

$$i_{Lm}(t) = \frac{(V_0 - V_{C2} - V_i)}{nL_m}(t - t_3) + i_{Lm}(t_3) \tag{8}$$

Mode 5 [$t_4 - t_0$]: This mode begins by turning ON switch S. The leakage inductor energizes quickly using the full magnetizing current while the parasitic capacitance across the switch

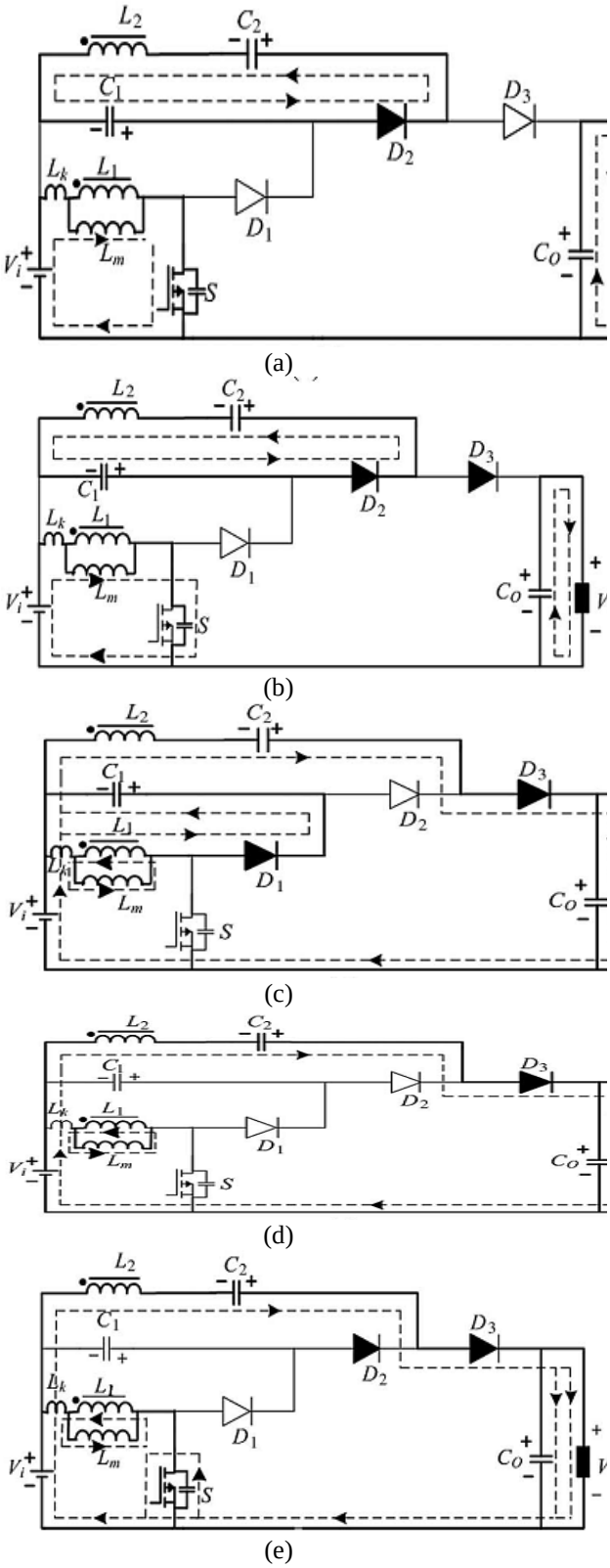

Fig.3. Various modes of operation during CCM: (a) Mode 1; (b) Mode 2; (c) Mode 3; (d) Mode 4; and (e) Mode 5.

discharges in this mode. The two diodes D1 and D2 are in reverse biased condition. The current flow path in this mode is shown in Fig.4(e). This mode ends when diode D3 becomes reverse biased and current flow through inductor L2 changes direction. The secondary inductor current (iLm) continues to flow in this mode and current is given by

$$i_{Lm}(t) = \frac{(V_0 - V_{C2} - V_i)}{nL_m}(t - t_4) + i_{Lm}(t_4) \quad (9)$$

Since the current through an inductor $\left(i_{lk} = \frac{V_i(t-t_4)}{(L_m+L_k)}\right)$ cannot change instantaneously, current rises slowly.

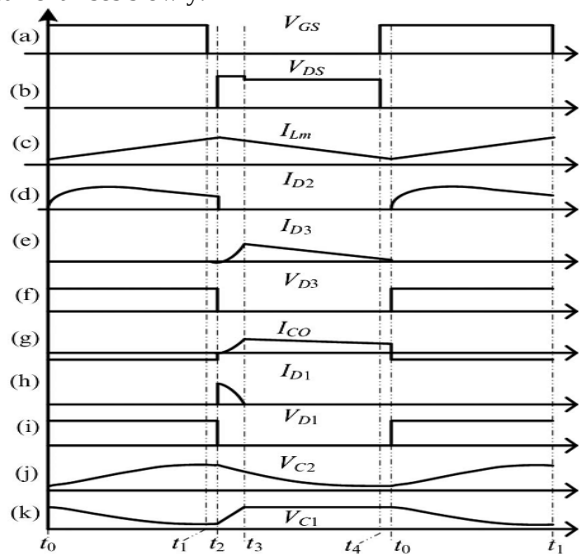

Fig.4. Typical waveforms during CCM operation

The voltage (VDS) across the switch "S" cannot change instantaneously and decreases slowly. Thus, there is little overlap of falling voltage and rising current and negligible switching loss at turn-ON. Typical waveforms of the circuit are shown in Fig.4.

4 ANALYSIS AND DESIGN

The analysis of the proposed converter which can be used for its design .All the elements used in the converter are assumed to be ideal. When switch S is ON: The voltage across L1 is given by

$$V_{L1(ON)} = V_i \tag{10}$$

The voltage across L_2 is given by

$$V_{L2} = V_{C2} - V_{C1}$$
$$V_{L2} = nV_i. \tag{11}$$

When switch S is OFF: The voltage across L_1 is given by

$$V_{L1(OFF)} = -V_{C1} \tag{12}$$

Applying Kirchoff's voltage law in Mode 3 yields

$$V_{L2} = V_i + V_{C2} - V_o. \tag{13}$$

By substituting VC2 from (11) and (12) into (13), it becomes

$$V_{L2} = V_i - V_{L1(OFF)} + nV_i - V_o \tag{14}$$

$$V_{L1} = \frac{V_{L2}}{n} \tag{15}$$

By substituting (14) into (15), voltage expression during switch OFF condition becomes

$$V_{L1(OFF)} = \frac{\left(V_i - V_{L1(OFF)} + nV_i - V_o\right)}{n}$$

Or,

$$V_{L1(OFF)} = \frac{(V_i + nV_i - V_o)}{(n+1)} \tag{16}$$

Voltage gain: By applying voltage-sec balance across L1,

$$V_{L1(ON)}d + V_{L1(OFF)}(1-d) = 0 \tag{17}$$

Substituting values of VL1(ON) and VL1(OFF) from (10) and (16), respectively, into (17) yields

$$V_i d + \frac{(V_i + nV_i - V_o)}{(n+1)}(1-d) = ($$

$$\frac{V_o}{V_i} = \frac{(n+1)}{(1-d)}. \tag{18}$$

Substituting (18) into (16) results in

$$V_{L1(OFF)} = -\frac{d}{(1-d)}V_i \tag{19}$$

Switch voltage: Voltage across the switch during OFF time is given by

$$V_{DS} = -V_{L1(OFF)} + V_i \tag{20}$$

Substituting (19) into (20) results in

$$V_{DS} = \frac{d}{(1-d)}V_i + V_i \tag{21}$$

$$V_{DS} = \frac{V_i}{(1-d)} \tag{22}$$

Again, the voltage across the clamp capacitor C1 is nearly constant for the entire switching period. Using (12) and (19),

$$V_{C1} = \frac{d}{(1-d)}V_i \tag{23}$$

Intermediate capacitor voltage (VC2): The voltage across intermediate energy storage capacitor would be nearly constant (negligible ripple) and can be determined from (11) as follows:

$$V_{C2} = V_{C1} + V_{L2} \tag{24}$$

By substituting (13) and (23) in (24),

$$V_{C2} = \frac{d}{(1-d)}V_i + nV_i \tag{25}$$

$$V_{C2} = \frac{d(1-n)+n}{(1-d)}V_i \tag{26}$$

Reverse bias voltage across diodes (VD1, VD2, VD3):

Voltage across diode (D1)

$$V_{D1} = V_{L1(ON)} + V_{C1} \tag{27}$$

By substituting (10) and (23) into (27), the voltage across diode D1 becomes

$$V_{D1} = \frac{V_i}{(1-d)} \tag{28}$$

Voltage across diode (D2) is

$$V_{D2} = V_{L2} + V_{C2} - V_{C1} \tag{29}$$

By substituting (13), (23), and (26) in (29), it becomes

$$V_{D2} = 2nV_i \tag{30}$$

Voltage across diode D3,

$$V_{D3} = V_{L2} - V_{C2} - V_i + V_o \tag{31}$$

By substituting the value of VL2 from (13), Vo from (18) and VC2 from (26) in (31) yield

$$V_{D3} = \frac{n}{(1-d)} V_i \tag{32}$$

Magnetizing inductance (Lm):

$$L_m = \frac{1}{2} \times \frac{V_i \times d}{d \times I_{Lm} \times f_s} \tag{33}$$

Forward bias diode currents (I_{D1}, I_{D2}, I_{D3}): Current flow through diode D_1 can be derived as follows:

$$L_1 \frac{dI_{D1}}{dt} = V_{C1}$$

$$I_{D1} = \frac{V_{C1} \times d_{lk}}{L_1 \times f_s} \tag{34}$$

where dlkTS is the period during which the leakage energy is transferred. Current flowing through diode D2 can be calculated as follows (S ON):

$$L_2 \frac{dI_m}{dt} = V_{C2} - V_{C1}$$

where Im = nI_{L2}; $I_{L2} = I_{D2}$

$$I_{D2} = \frac{(V_{C2} - V_{C1}) \times d}{n \times L_2 \times f_s} \tag{35}$$

Similarly, the current flowing through diode D_3 can be calculated as follows (S OFF):

$$L_2 \frac{dI_m}{dt} = V_o - V_{C2} - V_i$$

where Im = nIL_2; $I_{L2} = I_{D3}$

$$I_{D3} = \frac{(V_o - V_{C2} - V_i)(1 - d - d_{lk})}{n \times L_2 \times f_s} \tag{36}$$

The presence of leakage inductance in the circuit manifests itself in the following manner:

$$V_i = L_m \frac{di}{dt} + L_k \frac{di}{dt} \tag{37}$$

Then, current flowing through inductor becomes

$$i = \int \frac{V_i}{(L_m + L_k)} dt \tag{38}$$

From (38), it is clear that the current flowing through the circuit is reduced if leakage inductance is present

Also, $$V_{L1} = kV_i \tag{39}$$

where k is the coupling coefficient of the coupled inductor

$$V_{L2} = knV_i \tag{40}$$

By using (10)–(18) and taking into account the leakage inductance, voltage gain expression can be determined as

$$\frac{V_o}{V_i} = \frac{(nk+1) + d(k-1)}{(1-d)} \tag{41}$$

5 Proposed Work: Grid connected Inverter

A grid-tie inverter is a inverter that converts direct current (DC) electricity into alternating current (AC) with an ability to synchronize to interface with a utility line. Its applications are converting DC

International Journal of Research
Available at https://edupediapublications.org/journals
e-ISSN: 2348-6848
p-ISSN: 2348-795X
Volume 05 Issue 12
April 2018

sources such as solar panels or small wind turbines into AC for tying with the grid.

Residences and businesses that have a grid-tied electrical system are permitted in many countries to sell their energy to the utility grid. Electricity delivered to the grid can be compensated in several ways. "Net metering" is where the entity that owns the renewable energy power source receives compensation from the utility for its net outflow of power. So for example, if during a given month a power system feeds 500 kilowatt-hours into the grid and uses 100 kilowatt-hours from the grid, it would receive compensation for 400 kilowatt-hours. In the US, net metering policies vary by jurisdiction. Another policy is a feed-in tariff, where the producer is paid for every kilowatt hour delivered to the grid by a special tariff based on a contract with distribution company or other power authority.

In the United States, grid-interactive power systems are covered by specific provisions in the National Electric Code, which also mandates certain requirements for grid-interactive inverters.

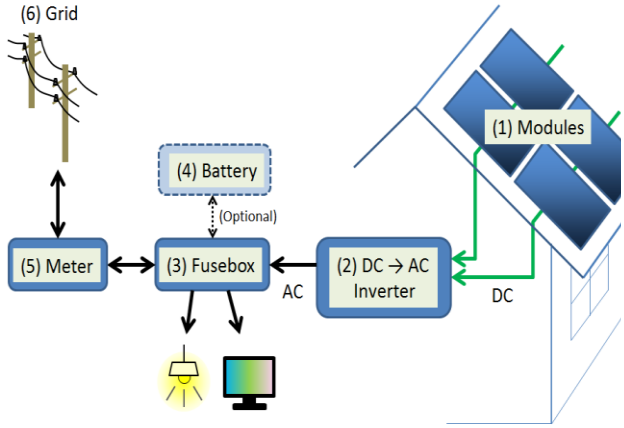

Fig 5.Grid connected PV inverter

A Operation:

Inverters take DC power and invert it to AC power so it can be fed into the electric utility company grid. The grid tie inverter (GTI) must synchronize its frequency with that of the grid (e.g. 50 or 60 Hz) using a local oscillator and limit the voltage to no higher than the grid voltage. A high-quality modern GTI has a fixed unity power factor, which means its output voltage and current are perfectly lined up, and its phase angle is within 1 degree of the AC power grid. The inverter has an on-board computer which senses the current AC grid waveform, and outputs a voltage to correspond with the grid. However, supplying reactive power to the grid might be necessary to keep the voltage in the local grid inside allowed limitations. Otherwise, in a grid segment with considerable power from renewable sources, voltage levels might rise too much at times of high production, i.e. around noon.

Grid-tie inverters are also designed to quickly disconnect from the grid if the utility grid goes down. This is an NEC requirement[2] that ensures that in the event of a blackout, the grid tie inverter will shut down to prevent the energy it transfers from harming any line workers who are sent to fix the power grid.

Properly configured, a grid tie inverter enables a home owner to use an alternative power generation system like solar or wind power without extensive rewiring and without batteries. If the alternative power being produced is insufficient, the deficit will be sourced from the electricity grid.

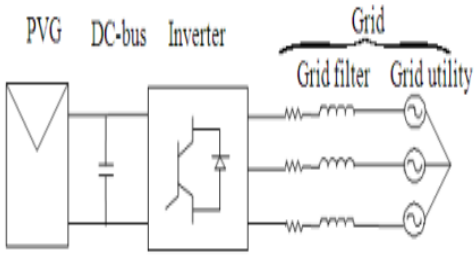

Fig 6 Typical configuration of a grid connected photovoltaic system

B Characteristics of Grid tied Inverter:

- ***Rated output power*:** This value is provided in watts or kilowatts. For some inverters, they may provide an output rating for different output voltages. For instance, if the inverter can be configured for either 240 VAC or 208 VAC output, the rated power output may be different for each of those configurations.
- ***Output voltage(s)*:** This value indicates to which utility voltages the inverter can connect. For smaller inverters that are designed for residential use, the output voltage is usually 240 VAC. Inverters that target commercial applications are rated for 208, 240, 277, 400, 480 or 600 VAC and may also produce three phase power.
- ***Peak efficiency*:** The peak efficiency represents the highest efficiency that the inverter can achieve. Most grid-tie inverters on the market as of July 2009 have peak efficiencies of over 94%, some as high as 96%. The energy lost during inversion is for the most part converted into

heat. Consequently, in order for an inverter to output its rated power it will require a power input that exceeds its output. For example, a 5000 W inverter operating at full power at 95% efficiency will require an input of 5,263 W (rated power divided by efficiency). Inverters that are capable of producing power at different AC voltages may have different efficiencies associated with each voltage.

- ***CEC weighted efficiency*:** This efficiency is published by the California Energy Commission on its Go Solar website. In contrast to peak efficiency, this value is an average efficiency and is a better representation of the inverter's operating profile. Inverters that are capable of producing power at different AC voltages may have different efficiencies associated with each voltage.
- ***Maximum input current*:** This is the maximum amount of direct current that the inverter can use. If a system, solar cells for example, produces a current in excess of the maximum input current, that current is not used by the inverter.
- ***Maximum output current*:** The maximum output current is the maximum continuous alternating current that the inverter will supply. This value is typically used to determine the minimum current rating of the over-current protection devices (e.g., breakers and fuses) and disconnects required for the output circuit. Inverters that are capable of producing power at different AC voltages will have different maximum outputs for each voltage.
- ***Peak power tracking voltage*:** This represents the DC voltage range in which the inverter's maximum point power tracker will operate. The system designer must configure the strings optimally so that during the majority of the year, the voltage of the strings will be within this range. This can be a difficult task since voltage will fluctuate with changes in temperature.
- ***Start voltage*:** This value is not listed on all inverter datasheets. The value indicates the minimum DC voltage that is required in order for the inverter to turn on and begin operation. This is especially important for solar applications, because the system designer must be sure that there is a sufficient number of solar modules wired in series in each string to produce this voltage. If this value is not provided by the manufacturer, system designers typically use the lower band of the peak power tracking voltage range as the inverter's minimum voltage.
- ***IPxx rating*:** The Ingress Protection rating or IP Code classifies and rates the level of protection provided against the ingress of solid foreign objects (first digit) or water (second digit), a higher digit means greater protection. In the US the *NEMA enclosure type* is used similarly to the international rating. Most inverters are rated for outdoors installation with IP45 (no dust protection) or IP65 (dust tight), or in the US, NEMA 3R (no windblown dust protection) or NEMA 4X (windblown dust, direct water splash and additional corrosion protection).

6 SIMULATION RESULTS

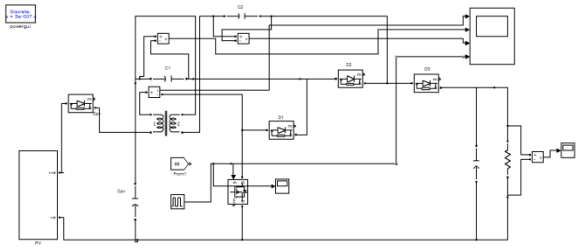

Fig.7 Simulation/Matlab diagram of a proposed high gain dc-dc converter.

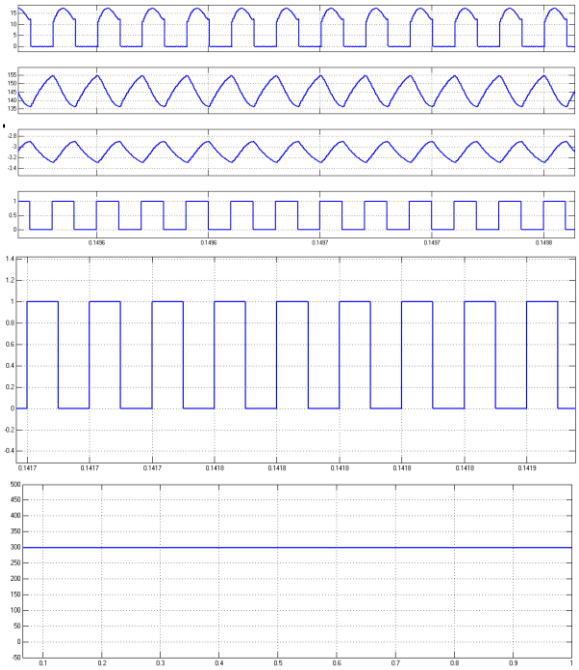

Fig 8 Waveforms of V_{GS}, V_{DS}, I_{LM}, I_D, V_D, I_{C0}

International Journal of Research
Available at https://edupediapublications.org/journals
e-ISSN: 2348-6848
p-ISSN: 2348-795X
Volume 05 Issue 12
April 2018

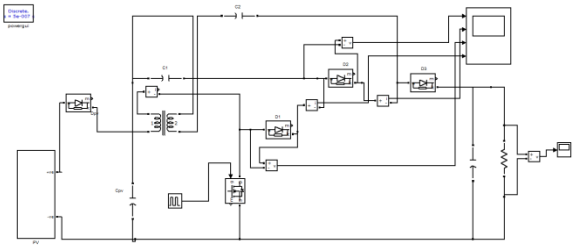

Fig. 9 Simulation/Matlab diagram of a proposed high gain dc-dc converter.

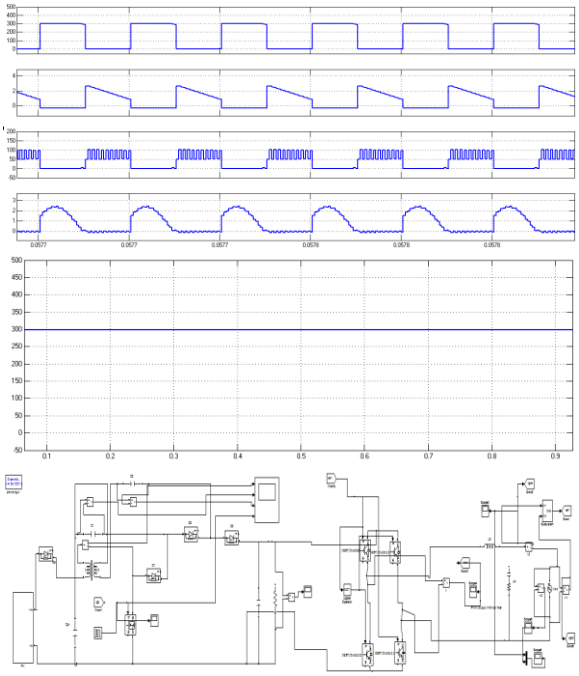

Fig.10 Simulation/Matlab diagram of a proposed high gain dc-dc converter with soft switching for inverter with grid connected unit.

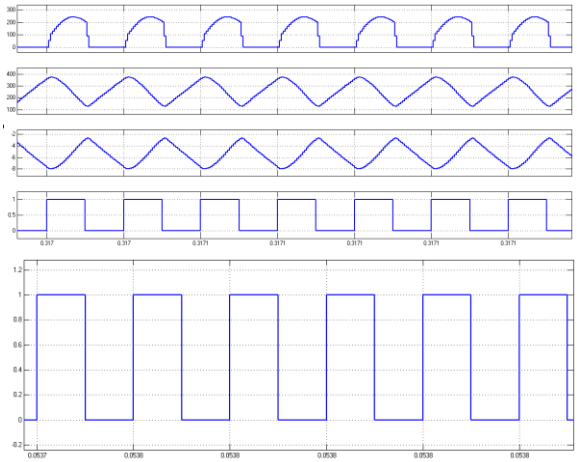

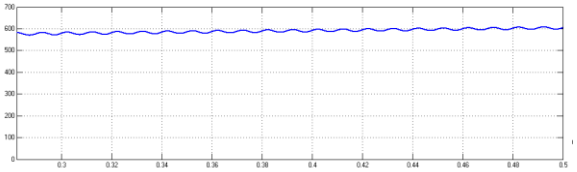

Fig 11 Waveforms of V_{GS}, V_{DS}, I_{LM}, I_D, V_D, I_{C0}

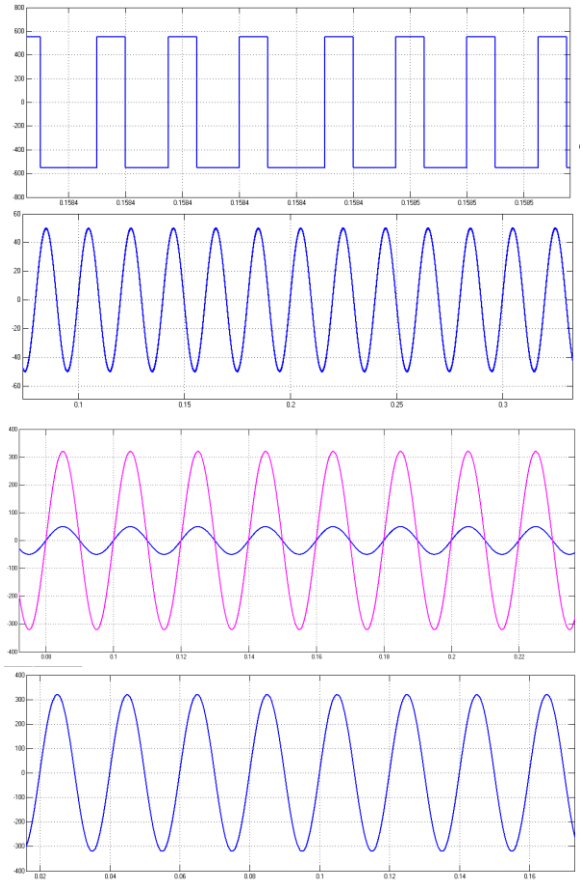

Fig 12 Waveforms of voltage and current

7 CONCLUSION

A soft switching for inverter with grid connected unit with high voltage gain has been proposed in this paper. The proposed converter can minimize the voltage stresses of the switching devices and lower the turn ratio of the coupled inductor. It provides a continuous input current, and the ripple components of the input current can be controlled by using the inductance of the CCM boost cell. Finally the proposed converter is applied in standalone renewable application. A Mat lab/Simulink model is developed and simulation results are presented.

REFERENCES

[1] W. Li and X. He, "Review of non-isolated high-step-up DC/DC converters in photovoltaic grid-connected applications," IEEE Trans. Ind. Electron., vol. 58, no. 4, pp. 1239–1250, Apr. 2011.
[2] E. Mamarelis, G. Petrone, and G. Spagnuolo, "Design of a slidingmode-controlled SEPIC for PV MPPT applications," IEEE Trans. Ind. Electron., vol. 61, no. 7, pp. 3387–3398, Jul. 2014.
[3] K. W. Ma and Y. S. Lee, "An integrated fly-back converter for DC uninterruptible power supply," IEEE Trans. Power Electron., vol. 11, no. 2, pp. 318–327, Mar. 1996.
[4] Q. Zhao and F. C. Lee, "High-efficiency, high step-up DC–DC converters," IEEE Trans. Power Electron., vol. 18, no. 1, pp. 65–73, Jan.2003.
[5] G. C. Silveira, F. L. Tofoli, L. D. S. Bezerra, and R. P. Torrico-Bascope, "A nonisolated dc–dc boost converter with high voltage gain and balanced output voltage," IEEE Trans. Ind. Electron., vol. 61, no. 12, pp. 6739– 6746, Dec. 2014.
[6] C. T. Pan, C. F. Chuang, and C. C. Chu "A novel transformer-less adaptable voltage quadrupler DC converter with low switch voltage stress," IEEE Trans. Power Electron., vol. 29, no. 9, pp. 4787–4796, Sep. 2014.
[7] J. H. Lee, T. J. Liang, and J. F. Chen, "Isolated coupled-inductor integrated DC–DC converter with nondissipative snubber for solar energy applications," IEEE Trans. Ind. Electron., vol. 61, no. 7, pp. 3337–3348, Jul. 2014.
[8] P. Xuewei and A. K. Rathore, "Novel bidirectional snubberless naturally commutated soft-switching current-fed full-bridge isolated DC/DC converter for fuel cell vehicles," IEEE Trans. Ind. Electron., vol. 61, no. 5, pp. 2307–2315, May 2014.
[9] C. T. Choi, C. K. Li, and S. K. Kok, "Modeling of an active clamp discontinuous conduction mode flyback converter under variation of operating conditions," in Proc. IEEE Int. Power Electron. Drive Syst. (PEDS), 1999, vol. 2, pp. 730–733.
[10] M. Prudente, L. L. Pfitscher, G. Emmendoerfer, E. F. Romaneli, and R. Gules, "Voltage multiplier cells applied to non-isolated DC–DC converters," IEEE Trans. Power Electron., vol. 23, no. 2, pp. 871–887, Mar. 2008.
[11] J. Xu, "Modeling and analysis of switching DC–DC converter with coupled-inductor," in Proc. IEEE Int. Conf. Circuits Syst. (CICC), May 12–15, 1991, pp. 717–720.
[12] A. F. Witulski, "Introduction to modeling of transformers and coupled inductors" IEEE Trans. Power Electron., vol. 10, no. 3, pp. 349–357, May 1995.
[13] F. S. Garcia, J. A. Pomilio, and G. Spiazzi, "Modeling and control design of the interleaved double dual boost converter," IEEE Trans. Ind. Electron., vol. 60, no. 8, pp. 3283–3290, Aug. 2013.
[14] P. W. Lee, Y. S. Lee, D. K. W. Cheng, and X. C. Liu, "Steady-state analysis of an interleaved boost converter with coupled inductors," IEEE Trans. Ind. Electron., vol. 47, no. 4, pp. 787–795, Aug. 2000.
[15] M. Kwon and B. H. Kwon, "High step-up active-clamp converter with input-current doubler and output-voltage doubler for fuel cell power systems," IEEE Trans. Power Electron., vol. 24, no. 1, pp. 108–115, Jan. 2009.
[16] K. C. Tseng and C. C. Huang, "High step-up high-efficiency interleaved converter with voltage multiplier module for renewable energy system," IEEE Trans. Ind. Electron., vol. 61, no. 3, pp. 1311–1319, Mar. 2014.
[17] S. Lee, P. Kim, and S. Choi, "High step-up soft-switched converters using voltage multiplier cells," IEEE Trans. Power Electron., vol. 28, no. 7, pp. 3379–3387, Jul. 2013.
[18] J. J. Jozwik and M. K. Kazimierczuk, "Dual sepic PWM switching-mode DC/DC power converter," IEEE Trans. Ind. Electron., vol. 36, no. 1, pp. 64–70, Feb. 1989.
[19] Y. P. Hsieh, J. F. Chen, T. J. Liang, and L. S. Yang, "Novel high step-up DC–DC converter for distributed generation system," IEEE Trans. Ind. Electron., vol. 60, no. 4, pp. 1473–1482, Apr. 2013.
[20] Y. J. A. Alcazar, D. S. Oliveira, F. L. Tofoli, and R. P. Torrico-Bascope, "DC–DC nonisolated boost converter based on the three-state switching cell and voltage multiplier cells," IEEE Trans. Ind. Electron., vol. 60, no. 10, pp. 4438–4449, Oct. 2013.

AUTHOR DETAILS

AUTHOR -1

SHABANA BEGUM
M-tech Student scholar
Department of Electrical &Electronics Engineering,
Institute Of Aeronautical Engineering (IARE),
Dundigal; Hyderabad (Dt), Telangana, India.
Email: shabana22614@gmail.com
Interested areas:Power electronics

AUTHOR -2

Dr. .P.MALLIKARJUN SHARMA

Professor
Department of Electrical & Electronics Engineering,
Institute Of Aeronautical Engineering (IARE),
Dundigal; Hyderabad (Dt), Telangana, India.
Email: p.mallikarjunsharma@iare.ac.in

AUTHOR -3

Professor and Head
Department of Electrical & Electronics Engineering,
Institute Of Aeronautical Engineering (IARE),
Dundigal; Hyderabad (Dt), Telangana, India.
Email: sridhar@iare.ac.in